Nuclear Instruments and Methods in Physics Research B 574 (2026) 166080

Contents lists available at ScienceDirect

Nuclear Inst. and Methods in Physics Research, B

journal homepage: www.elsevier.com/locate/nimb

Full Length Article

A new experimental system for studying defects and deuterium lattice location in single crystals by ion beam Methods☆

Esther Punzón-Quijorna *, Mitja Kelemen, Roberto Galende-Pérez, Primož Vavpetič, Primož Pelicon, Sabina Markelj

Jožef Stefan Institute (JSI), Ljubljana, Slovenia

ARTICLE INFO

Keywords:
Channeling
RBS
NRA
Deturerium
Tungsten
Fusion
Goniometer

ABSTRACT

A high-precision 5-axis goniometer has been installed and commissioned at the INSIBA end station of the 2 MV Tandetron accelerator at the Jožef Stefan Institute. The system provides three translational and two rotational degrees of freedom with an angular resolution of 0.01°, enabling precise sample alignment for Rutherford Backscattering Spectrometry (RBS-C) and Nuclear Reaction Analysis (NRA-C), both in channeling mode. The goniometer is equipped with a versatile sample stage allowing continuous heating up to 1470 K, liquid-nitrogen cooling, and biasing up to 500 V. A load-lock system ensures vacuum integrity during sample exchange. The system supports simultaneous data acquisition from up to five detectors.

Commissioning was performed using pristine and W-ion irradiated W(111) single crystals by 10.8 MeV W ions inducing damage of 0.02 and 0.2 dpa at RT, as well as D-plasma-exposed W(100) crystals containing deuterium-decorated defects. Simultaneous RBS-C and NRA-C measurements demonstrated consistent results with benchmark data, confirming the system's precision and stability. The setup also enables in-situ RBS-C during thermal annealing, facilitating real-time studies of defect recovery and hydrogen behaviour. This system represents a major enhancement in ion beam analysis capabilities for investigating defect dynamics and light element trapping and transport in materials.

1. Introduction

Ion beam analysis (IBA) techniques have long been recognized as powerful, non-destructive tools for characterizing the structural and compositional properties of materials with high precision. In particular, Rutherford Backscattering Spectrometry (RBS-C) and Nuclear Reaction Analysis (NRA-C), both in channeling mode, provide unique sensitivity to lattice disorder and allow the determination of light element distributions within a crystal lattice. The channeling effect arises when an ion beam is aligned with a major crystallographic axis or plane, resulting in a reduced backscattering yield from well-aligned atomic rows. Deviations from this ideal channeling condition, caused by lattice defects or impurity atoms occupying non-substitutional sites, lead to measurable increases in the backscattering yield.

In RBS-C, the angular dependence of backscattered ions reveals information about lattice alignment and atomic displacement, enabling quantitative determination of crystal quality and defect density [1]. When combined with NRA-C, which offers isotopic and elemental sensitivity for light atoms such as hydrogen, deuterium, or carbon, a more complete understanding of defect-impurity interactions can be obtained. As a result, RBS-C and NRA-C are complementary tools for studying both defect structures and impurity lattice locations at the atomic scale. These techniques exploit the sensitivity of ion-channeling phenomena to the crystalline order of the target material, allowing the study of defect formation, migration, and recovery with atomic-scale resolution.

Accurate implementation of these channeling techniques requires precise sample alignment relative to the incident ion beam and detector geometry. Even small angular misalignments can significantly affect the measured channeling yield and compromise data reliability. To overcome these limitations, high-precision multi-axis goniometers are employed to ensure accurate orientation control of single-crystal samples during measurement [2]. Such systems are essential not only for minimizing alignment errors but also for enabling advanced

☆ This article is part of a special issue entitled: '2025 IBA ? PIXE' published in Nuclear Inst. and Methods in Physics Research, B.

* Corresponding author.
E-mail address: esther.punzon-quijorna@ijs.si (E. Punzón-Quijorna).

https://doi.org/10.1016/j.nimb.2026.166080
Received 17 December 2025; Received in revised form 2 March 2026; Accepted 6 March 2026
Available online 13 March 2026

measurement such as in-situ thermal annealing, dynamic defect recovery studies, and simultaneous multi-detector data acquisition.

In this context, a high-precision five-axis goniometer has been installed and commissioned at the INSIBA end-station of the 2 MV Tandetron accelerator at the Jožef Stefan Institute (JSI), Ljubljana, Slovenia. The goniometer is a device that enables to displace and rotate the sample. It consists of a mechanical arm and a rotating plate where the samples are placed. It gives five degrees of freedom: the three spatial ones (provided by the mechanical arm) and the two angular ones (two rotations around the two spatial axes). This flexibility enables us to perform an accurate linear scan when searching for the channels of the sample.

The commissioning of this new system was carried out using tungsten (W) single crystals, a relevant material of central importance for nuclear fusion applications. Tungsten is considered as a prime candidate for plasma-facing components in next-generation fusion devices due to its high melting point and thermal conductivity, low sputtering yield, and low hydrogen isotope (HI) retention. However, under the extreme conditions present in fusion reactors, tungsten is exposed to intense particle bombardment by hydrogen isotopes, 14 MeV neutron irradiation, and high heat flux. Neutron bombardment leads to the formation of irradiation-induced defects such as vacancies, dislocation loops, and voids, which act as trapping sites for hydrogen isotopes and alter their mobility and retention.

Understanding the behaviour of defects and hydrogen isotopes (HI) in metals, particularly tungsten (W), is crucial for the development of materials capable of resisting the harsh environments found in nuclear fission and fusion reactors. Structural defects, such as vacancies, dislocations, and grain boundaries significantly influence the mechanical and thermal properties of metals. These defects may lead to embrittlement, swelling, impurity segregation, and degradation of thermal and electrical conductivity, phenomena which directly affect the performance and lifetime of reactor components.

To reproduce and study such effects under controlled laboratory conditions, heavy-ion irradiation with MeV self-ions is frequently employed as a surrogate for neutron-induced damage [3 4]. Both neutron and ion irradiation involves the creation of a primary knock-on atom (PKA) which is knocked out of its position with a significant energy transfer. This energetic particle then causes further displacement damage in the material and is, therefore, responsible for the majority of the displacement damage created during a neutron impact. This approach allows systematic exploration of defect production, recovery, and interaction with implanted hydrogen isotopes, without the complications associated with material activation, helium production and transmutation. The combination of RBS-C and NRA-C provides a particularly effective framework for these investigations: RBS-C quantifies lattice disorder and defect accumulation, while NRA-C reveals the spatial distribution of light elements such as deuterium or tritium within the damaged regions [5]. Performing these techniques simultaneously enables direct correlation between defect evolution and hydrogen isotope trapping [6].

The commissioning experiments reported here were performed on pristine and 10.8 MeV W-ion-irradiated W(111) and W(100) single crystals to validate the mechanical precision and analytical capability of the new goniometer system. RBS-C and NRA-C measurements were used to probe lattice disorder and deuterium distribution in ion-damaged tungsten. The results confirmed excellent reproducibility and alignment precision, as well as the system's capability for in-situ channeling measurements during thermal annealing.

2. Experimental

2.1. Goniometer and beamline upgrade

The five-axis goniometer has been installed at the INSIBA end-station, located at + 10° of the switching magnet on the 2 MV tandem accelerator at JSI. The goniometer was manufactured by Thermionics Laboratory Inc. (TLI) and purchased together with the National Electrostatic Corp. (NEC) goniometer manipulator and data acquisition system. Fig. 1 shows the picture of the goniometer (in red color) installed on top of the INSIBA vacuum chamber. This new setup offers three translational (x, y, and z) and two rotational axes (polar and tilt) with a precise angular resolution of 0.01°, allowing the sample to be positioned at the proper angle (crystallographic orientation) to perform channeling measurements. Fig. 2 shows a photo of the goniometer where we can see the linear and angular manipulators (a), and the sample holder, thermocouple and heater (below the sample plate) (b). The 3 translational axes (x, y, and z) and three rotational axes (azimuthal, polar and tilt) are showed in c), together with the direction of the beam (green arrow). Unfortunately, the tilt and azimuth axes were initially mechanically coupled, making it impossible to adjust the tilt angle while keeping the azimuth angle fixed. As a result, any change in the tilt angle also altered the azimuth angle and therefore consequently changing the sample position with respect to the beam. This coupling prevented accurate channeling location using polar and tilt scans, since the azimuthal position could not be independently controlled. Due to this manufacturing defect, the azimuth axis had to be disabled, reducing the goniometer from a 6-axis to a 5-axis system.

The sample holder consists of 74.7 mm (2.94 in.) sample transfer platen with a smaller 50.8 mm (2 in.) removable platen, both made out of Mo. This enables us mounting of several samples at once. The transfer platen incorporates transferable K-type thermocouple hot junction and is mounted on a frame where nude W filament heater for ultra-high vacuum applications is embedded for 2 in. sample plate. The sample platen has a K-type thermocouple attached to the front surface which enables sample temperature measurement and control. The heater provides sample platen heating to 1200 °C continuous and includes ceramic insulated power leads from the heater to vacuum feedthrough and type K reference thermocouple with ceramic insulated wires to vacuum feedthrough. The heater came with a radiant resistive heater power supply 240 V AC, 50/60 Hz input voltage with Eurotherm PID automatic temperature control with auto tuning and digital temperature read-out. The whole system is galvanically decoupled from the rest of the system which enables sample bias up to 500 V. The system is designed such that the mean rotational surface axis is on 1.5 mm thick sample surface.

The whole system is cooled with liquid nitrogen vapour cooling, which has been tested for cooling down the samples to 170 K so far. The system cooling needs to be provided also when high-temperature heating is applied. This liquid cooling option allows rapid cooling of the samples after stopping irradiation at high temperatures and enables the study of radiation effects in materials down to liquid nitrogen temperatures. The goniometer was purchased together with a load-lock chamber to maintain vacuum integrity during sample exchange. The combined NEC system supports up to five detectors for simultaneous spectra acquisition and manipulation of the sample position during the data collection.

Inside the INSIBA chamber, two detectors were placed. The backscattered ^{3}He or ^{4}He ions were collected using the so-called RBS detector, which is a 300 μm thick Partially depleted Passivated Planar Silicon (PIPS) detector by Canberra with 50 mm^2 active area. It was located 135 mm from the target at an angle of 165° with respect to the incoming beam covering a geometrical solid angle of 0.7 msr ± 0.02 msr. A second 1500 μm thick PIPS detector, also by Canberra, with 300 mm^2 active area, the so-called NRA detector, was placed at a 135° scattering angle. The detector had a circular aperture with a diameter of 19.54 mm and was positioned 104 mm from the target, covering a geometrical solid angle of 26.69 msr ± 0.12 msr. The NRA detector is capable of fully stopping protons from the D(^{3}He,p)^{4}He reaction, thus enabling the absolute quantification of deuterium. A 24 μm Al absorber was placed in front of the detector to stop the backscattered ^{3}He ions.

Due to the long beamline there is an electrostatic quadrupole lens

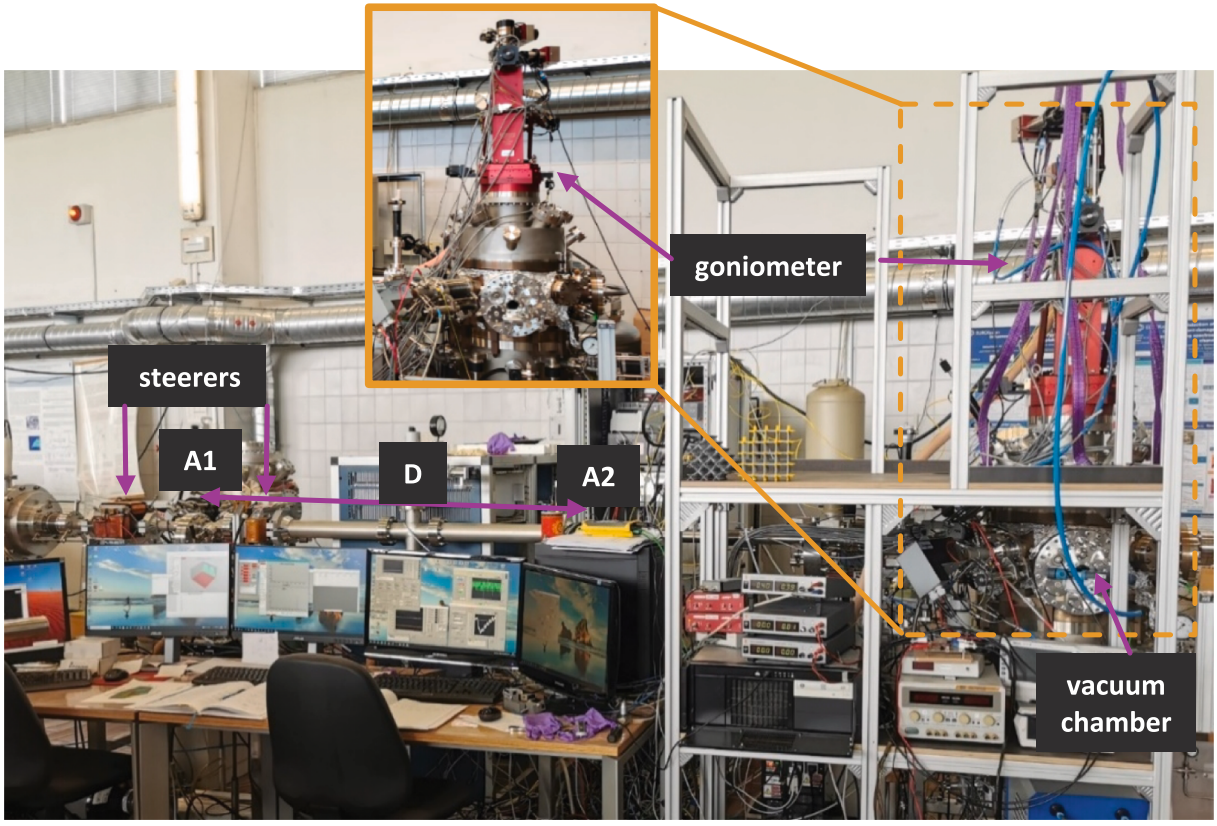

Fig. 1. Photo of the end of the 10° beamline with INSIBA vacuum chamber and the 5-axis goniometer (on the top, in red colour). The steerers and apertures (A1 and A2) are also showed.

placed 4.5 m before the experimental chamber in order to gather the beam. Together with the goniometer, some additional upgrades have been introduced in the beamline in order to improve manipulation and achieve the proper divergence of the beam. As shown in Fig. 1, two sets of magnetic steerers were introduced to optimise and control the beam position and size. In order to improve the divergence of the beam the two slits, labelled as A1 and A2 in Fig. 1, previously separated by 1 m distance, were moved to a distance, D, of 2.5 m. This new arrangement allowed us to go from minimum RBS-C yield values of 20% down to 2–3%, with the same crystalline sample.

The beam current was measured by the ion mesh charge collector [7] with a 77.4% geometrical transmission and a bias of 600 V. The mesh charge system is placed just in front of the vacuum chamber after the second slit, A2.

2.2. Sample preparation

First tests were performed on W single crystals with (111) and (100) surface orientations, before already studied in [8,9] and [10], respectively. The W single crystals with (111) surface orientation were chosen due to their widest channeling axis based on [11]. W(111) samples (purchased at Surface Preparation Laboratory B.V) had a purity of 99.999% and a surface normal aligned with an accuracy $< 0.4°$. The top surface was polished to a roughness < 30 nm and shaped into a model SPL.EU.19 (diameter of 12 mm, thickness of 1.5 mm and a side groove of 1 mm). A 0.6 mm thermocouple hole facilitated accurate temperature measurements. Sample surface preparation before W irradiation was detailed in [9].

The combined RBS-C and NRA-C was performed on W(100) single crystals [10], with purity of 99.999%, purchased at MaTecK. Those had dimensions of 1x10x10 mm^3 and a surface normal orientation with an accuracy of $< 0.1°$. The top surface was purchased to be polished to an average roughness < 10 nm. W(100) single crystal was used in this case since the deuterium location could be easier resolved whether to be close to octahedral or tetrahedral interstitial site [12].

Both sets of crystal orientations were analysed by scanning electron microscopy (SEM) to evaluate surface integrity. Metallographic preparation may introduce plastic deformation in the near-surface crystal structure, which can affect ion-channeling analysis and is visible using electron-channeling pattern (ECP) technique. Sample preparation, including chemo-mechanical vibration polishing followed by controlled annealing, was performed at Max-Planck Institute for Plasma Physics (IPP), Garching, Germany as detailed in [8,9]. Post-preparation, samples went under ECP analysis to ensure that the distorted layer has been removed.

In order to introduce damage with certain type of defects, as explained in detail in [9], samples were self-irradiated using 10.8 MeV W ions with W fluence of 5.8×10^{16} W/m^2 and 5.8×10^{17} W/m^2, at room temperature and at 800 K. With a displacement energy of 90 eV and a surface binding energy of 0 eV using SRIM calculation, this induces damage doses of 0.02 dpa and 0.2 dpa, predicting a displacement-damaged zone in W extending down to 1.3 μm. During irradiation, samples were tilted to avoid implantation in channeling orientation [8,9].

The self-irradiated W(100) single crystal samples were exposed to D plasma with energy of 5 eV, for 48 h at 370 K sample temperature [10]. In this way, no additional damage was introduced. The ion flux was 6.10^{19} D/m^2s, with a total ion fluence of 1.10^{25} D/m^2. This fluence was enough to populate the defects with deuterium throughout the whole damage depth.

2.3. RBS-C and NRA-C measurements

For all measurements, either for RBS-C or NRA-C, a duoplasmatron

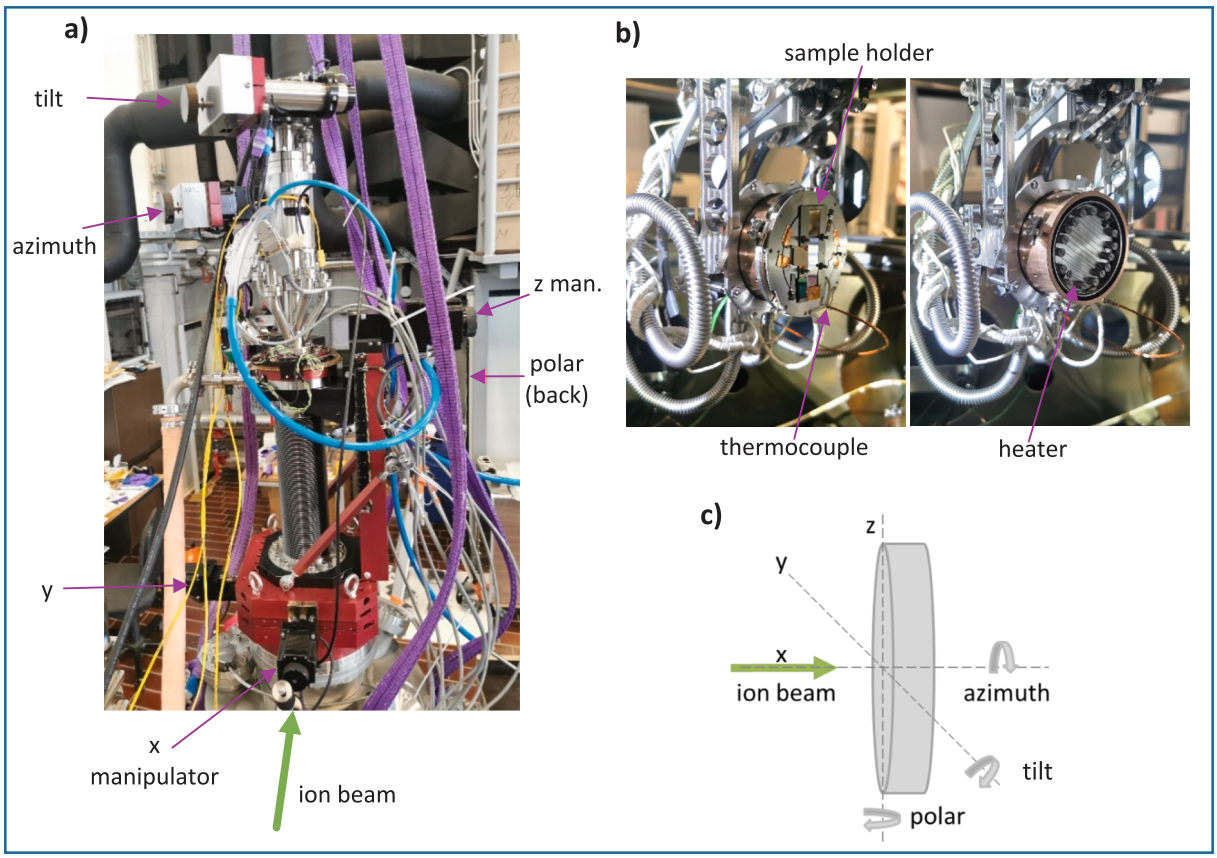

Fig. 2. a) in-detail photo of the goniometer showing the x-y-z linear and polar-azimuth-tilt angular manipulators. b) picture of the sample holder, thermocouple, and heather (below the sample plate). c) scheme showing the linear and angular directions. the green arrow shows the direction of the beam towards the sample in both cases.

ion source equipped with a lithium charge exchange channel was used to produce negative He ions. Helium negative ions (He^-) are selected by mass at the low-energy analysing magnet and then injected into the accelerator, and accelerated towards the positive terminal voltage. At the terminal the ions pass through a chamber with a stripper gas which removes electrons and converts them into positive ions. These positive ions are then repelled by the positive terminal and accelerated towards the ground potential. Finally, the switching magnet, at the exit of the accelerator, selects ions based on their energy and mass, filtering out unwanted species, and directing the selected ion species toward the INSIBA chamber, where the samples are positioned on the goniometer plate inside a vacuum chamber.

For the study of disorder in the samples, only RBS-C was applied using ^{4}He beam. For these measurements, we used $^4He^{2+}$ ion beam with 4.5 MeV energy. The procedure for finding the axial channeling orientation consisted of performing linear scans ranging from -3° to $+3^\circ$ (step size 0.1°) for polar or tilt angles, keeping the other one fixed, and repeating the process until the crystallographic orientation associated with the minimum backscattered yield is found. In this way, we have identified the values of polar-tilt where the minimum yield is measured. For each point we collected 30 nC. This method avoids unnecessary additional irradiation of the sample. Once the channel was found the RBS spectra were recorded in the axial channel. To collect the non-oriented (so-called random) spectrum, the sample was tilted to 6° out of the channel; the spectrum was then recorded while changing the polar angle from -3° to $+3^\circ$. Energy calibration of the RBS detector was made using several bulk polycrystalline targets.

For the study of D location on the material, we used ^{4}He beam to find the axial channel, and later the ^{3}He beam was used where RBS-C and NRA-C measurements are applied simultaneously. The D(^{3}He, p)^{4}He nuclear reaction was used [13]. After finding the conditions for axial channel using ^{4}He beam with 4.5 MeV energy, the samples were angular scanned along polar angle while both RBS-C and NRA-C spectrum were collected using ^{3}He beam at 1 MeV or 0.8 keV. A polar scan of +/- 3° was performed around the previously identified channeling conditions; the step was set to 0.1° with an accumulated charge of 300 nC per step.

2.4. RBS-C measurements during in-situ annealing

Annealing is used to remove radiation damage through the rearrangement and interaction of defects. The diffusion of defects is a thermally activated process. To study this phenomenon, we need to measure the RBS spectrum at different temperatures. The new goniometer sample holder allows recording of the RBS-C signal while the samples are heated, enabling the study of defect evolution.

To perform the measurements, the heater was PID controlled in order to linearly heat the sample, and sample temperature is in the feedback control loop. During the first test without a sample, we manually increased the heating power and monitored the pressure in the vacuum chamber to ensure it remained below 10^{-5} mbar. We observed that when the current was increased, the pressure rose rapidly at first and then continued to increase more slowly until a maximum value. Small current increases of 50 mA were sufficient to increase the temperature by more than one hundred degrees between room temperature and 500 °C, 770 K. We also found that the temperature difference between the heater and the sample surface was approximately 80 K. After the first test of the heater, the heating rate could be controlled with the Eurotherm controller. We could program the heating rate and hold time. We have programmed the heater to linearly heat the sample with a ramp of 5 K/min. Three measurements were taken during linear heating of the

sample, with a dose of 6.8 μC each, while heating. During these processes, active cooling was required. The sample was then cooled-down, and a new spectrum was recorded. Once it had completely cooled, a fifth and final spectrum was acquired.

3. Results

3.1. Benchmark validation

To evaluate the performance of our new set up, we replicated some of the measurements previously performed at the Centre for Microanalysis of Materials, CMAM, in Madrid, Spain on the same samples as used there, only newly re-polished and W-irradiated. In both cases, a 4.5 MeV $^{4}He^{+2}$ beam was used for the analysis.

In order to even get good channeling conditions the beam divergence had to be minimized. Optimum channeling conditions obtaining still reasonable beam current on the sample were achieved with the slits opening of 2 mm for the first one and 1.5 mm in diameter for the second one, details described in [14].

The channeling effect arises when an energetic ion beam is aligned with specific crystallographic directions of a single crystal. In this orientation, the ions experience a series of correlated, small-angle scattering events with the atomic rows or planes, rather than direct collisions with atomic nuclei. As a result, the ions are effectively "channeled" between atomic rows, penetrating deeper into the crystal with significantly reduced backscattering yield compared to a random orientation. This pronounced sensitivity of the backscattering yield to lattice alignment forms the basis of channeling analysis. In a perfect crystal (pink open circles and cyan close squares in Fig. 3), the low backscattering yield reflects the high degree of atomic order. However, when the lattice is disturbed by defects, displacements, or implanted impurities, the channeling condition is locally broken, allowing ions to interact more strongly with displaced atoms. Consequently, the backscattering yield increases in proportion to the amount of lattice disorder. The yield for the random orientation is the highest compared to the samples oriented in the channeling direction, since it is considered as a non-aligned material with a huge quantity of scattering centres. Such a spectrum is also obtained when a classical RBS spectrum is recorded on a polycrystalline W. The conversion from yield/channel to yield/depth was performed using the surface approximation. The depth scale was cross-validated in previous works [8 9] using transmission electron microscopy (TEM) cross-sections.

Before we could make a comparison between the spectra measured in Madrid and in our laboratory we had to normalize the spectra to the same particles × steradian. In Madrid, the accumulated dose was 12 μC, while In Ljubljana, it was 6.8 μC. Additionally, the solid angles covered by the detectors were not the same. To enable a proper comparison between the two datasets, we simulated both random spectra using SIMNRA [15] to obtain the number of particles × steradian for each spectrum. This yielded to a conversion factor Madrid/Ljubljana of 6.29 that allowed us to normalize the spectra. Fig. 3 shows the RBS measurements obtained in Madrid, previously published [4] (square markers), and the results obtained at JSI (open circle markers) using our new setup, on pristine and self-irradiated W(111) samples to 0.2 dpa at 290 K. Using 4.5 MeV He^{2+} on pristine and 0.2 dpa W(111) samples, our spectra matched closely to those measured in Madrid. However, as it can be noticed by the statistics in the signals is not the same.

After normalization, the agreement of the measured spectra are excellent for the pristine sample. Further, we were even able to obtain slightly better channeling with the new setup at JSI, as it can be seen in the lower yield for the pink open circles (marked "JSI channel"). The RBS spectrum for the W-irradiated sample differ to some extent but still show the same trend of increase in damage. The difference could be steaming from the defects in the sample, since the sample was newly W-irradiated for these measurements. On upper x axis the energy scale was transferred to a depth scale. The depth scale is estimated on the basis of the stopping power from SRIM with surface energy approximation [16]. The RBS spectra for both measurements change the slope at the same energy or depth, which is about 1.2 μm. There, the slope of the spectrum decreases and approaches that of the spectrum of the pristine W. This is the so-called 'knee point', where the first high-energy yield is due to ions backscattering directly from the displaced atoms in the sample and after that the signal is due to dechanneling [17].

We have also studied the effect of crystal orientation on damage distribution by analysing the RBS-C signals on two W single crystal set of samples with (111) and (100) crystal orientation. Namely, from recent theoretical calculations [18] it was shown that the loop orientation in relation to the RBS channeling direction affects the RBS-C results dramatically, where some loops are almost invisible and others yield a very high signal.

In Fig. 4 we have compared the RBS-C spectrum obtained from four

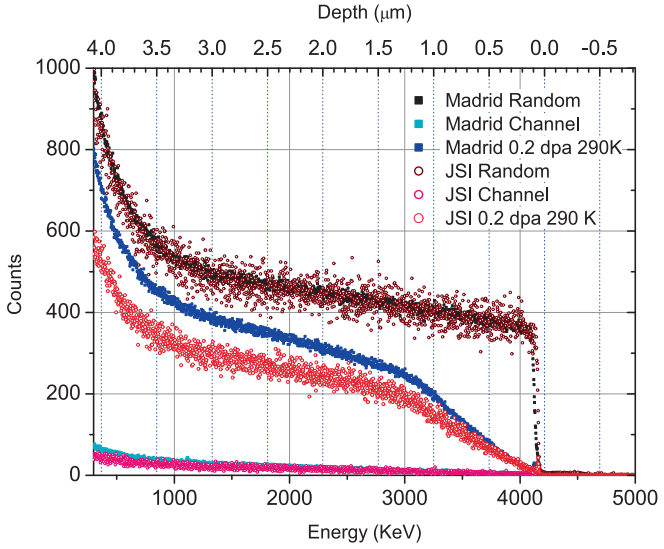

Fig. 3. 4.5 MeV He^{+2} RBS normalized signals. Comparison of random spectrum and spectra obtained in < 111 > axial channel for W sample irradiated up to 0.2 dpa at 290 K, and pristine sample with previous measurements performed in Madrid.

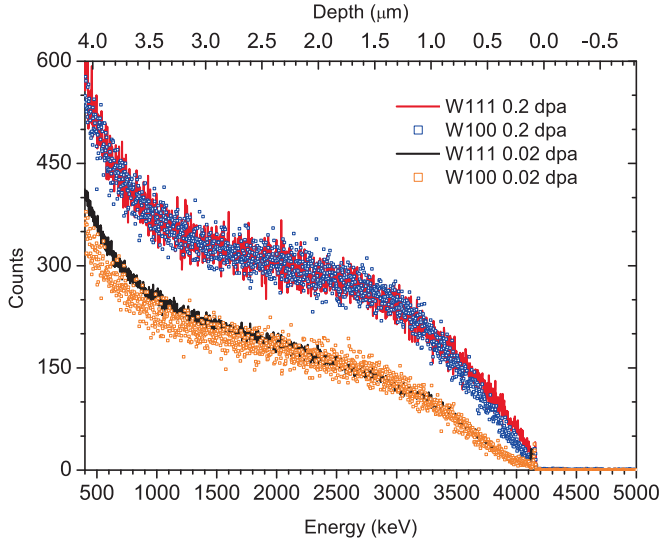

Fig. 4. RBS spectra in channeling configuration for four samples of W with orientations (111) and (100), and 0.2 and 0.02 dpa. All irradiated at 290 K. The black slid line measured on W(111) sample with 0.02 dpa, 290 K was measured in Madrid [8].

samples: two W(111) crystals, self-irradiated using 10.8 MeV W ions to doses up to 0.02 and 0.2 dpa; and two W(100) crystals irradiated with the same energies and doses. All samples were irradiated at 290 K. For the high dose level (0.2 dpa) (red line and blue open squares in Fig. 4), the RBS-C yield is the highest and no change in the yield is observed for the two different surface orientations. Both W(111) and W(100) have the same shape, which means that in either direction, the damage is the same, or in other words, the defect number and orientation is the same. This can mean that we have reached a saturation level in which defects have no longer preferential orientation. A similar behaviour has been observed for the lower dose, 0.02 dpa (orange squares and black line). In this case, we have compared our measurements on W(100) with 0.02 dpa, 290 K with the measurements from Madrid (black line) on the W (111) sample.

3.2. Simultaneous RBS-C and NRA-C measurements

When we are interested about the location of deuterium in the lattice one does not plot the whole spectra as shown above but we plot the RBS and NRA integrated signal as a function of angle, the so-called angular scan [1].

Fig. 6 shows the angular scans for two self-irradiated W(100) samples up to 0.02 dpa at 290 K (a) and 0.2 dpa at 800 K (b), and decorated with deuterium as previously described. Here we compare the results obtained at Helmholtz-Zentrum Dresden-Rossendorf (HZDR), in Dresden, Germany, published in [10]. It is important to note that the high-energy protons (12–13 MeV) from the nuclear reaction deposit in our NRA detector the whole energy, and the RBS signal is collected with a separate detector. This was not the case in the measurements at HZDR, where protons from NRA deposited only part of their energy in about 350 μm thick silicon detectors, and both RBS and NRA signals were collected with the same detector. The difference in RBS and NRA yield is several orders of magnitude, which makes data acquisition complicated due to the possible overlap of the signals [10]. As indicated in the figure, some angular scans are obtained from the 2D maps (polar-tilt scans) obtained at HZDR [10], while the results from JSI are all obtained from angular scans. All the signals are normalized and the error bars for NRA signals are included. Even with the lower statistics for the scans obtained from 2-D maps at HZDR, we can confirm that the trend is very similar. We can again observe that, where the RBS signal attains its minimum, the NRA signal has a peak. We can see that the peak for 0.2 dpa, 800 K (Fig. 5 b) has a wider and higher NRA-C signal compared to 0.02 dpa, 290 K (Fig. 5 a).

Our speculation for the difference, as was already stated for the initial measurements, is that since the vacancy clusters are larger in 0.2 dpa, 800 K sample (up to 50 vacancies in a cluster), as compared to the 0.02 dpa, 290 K sample (dominant divacancies) [9,10], the deuterium location in the larger vacancy clusters shows a broader distribution compared to that in smaller vacancy clusters.

3.3. In-situ annealing RBS-C measurements

The defect evolution during annealing was studied using a ^{4}He beam at 4.5 MeV by collecting the RBS-C spectra along the < 111 > axial channeling direction, while a continuous heating ramp with 5 K/min was applied. The study was performed on the sample that had the largest damage of 0.2 dpa at 290 K. Previous analysis of this sample [9] revealed a high density of dislocation lines and networks as the primary visible defects.

Each spectrum acquisition lasted approximately 15 min, corresponding to a temperature increase of about 75 K per measurement. The heating ramp is shown in Fig. 6. Five spectra were recorded and labelled according to the mean temperature during their acquisition (see Fig. 6). For clarity, the data points in all spectra were decimated by a factor of three.

When reaching 820 K, the RBS-C spectra could not be collected at higher temperatures due to increased noise in the RBS spectrum, which rendered measurements unreliable above approximately 790 K. At 820 K, the heater was switched off, and the sample was allowed to cool down. The increase in the RBS signal was attributed to the light sensitivity (photons) of the PIPS detector originating from the heater glow, rather than a change in the yield of the backscattered alpha particles.

There could be also an effect due to the temperature increase; however, the PIPS detector itself is kept at a constant ambient temperature by placing it at a sufficient distance (135 mm) from the sample, and by encapsulating it in an aluminium case to prevent temperature increase. From previous in situ experiments, we have shown that raising the sample temperature up to 800 K did not result in any change in the RBS spectrum [19 20]. The only difference was that, in that case, a 0.8 μm thick Al foil covered the detector.

When interpreting the RBS-C spectra obtained during the annealing, two opposing effects must be considered. On the one hand, increasing temperature enhances atomic vibrations, which raises the probability of ion interactions with lattice atoms, thereby reducing the channeling effect and increasing the RBS-C yield. On the other hand, elevated temperatures promote defect recovery processes that improve the crystal order, enhance channeling, and thus decrease the RBS-C yield.

A comparison between the room-temperature (RT, black) and 510 K (red) spectra reveals an increase in the RBS-C yield, which can be attributed to enhanced thermal vibrations of the lattice atoms. The spectrum collected at 670 K (blue), shows a significant decrease in RBS-C yield, which may indicate ongoing defect recovery and better

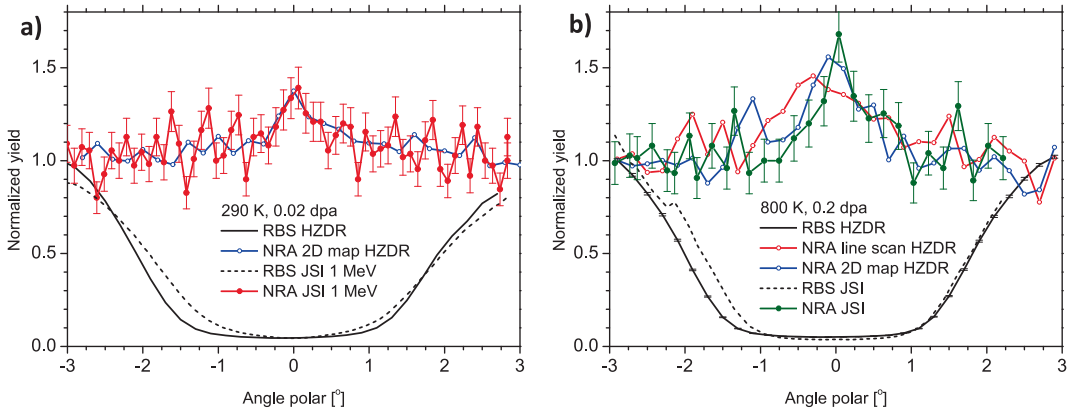

Fig. 5. Normalized RBS and NRA yields as a function of polar angle are shown for W(100) single crystal samples self-irradiated a) at 290 K and 0.02dpa, and b) at 800 K at 0.2 dpa. Comparison between measurements obtained at HZDR from [6] measured at 0.8 MeV ^{3}He energy and measurements obtained at JSI obtained with 1 MeV ^{3}He energy for 0.02 dpa, 290 K sample and with 0.8 MeV ^{3}He energy.

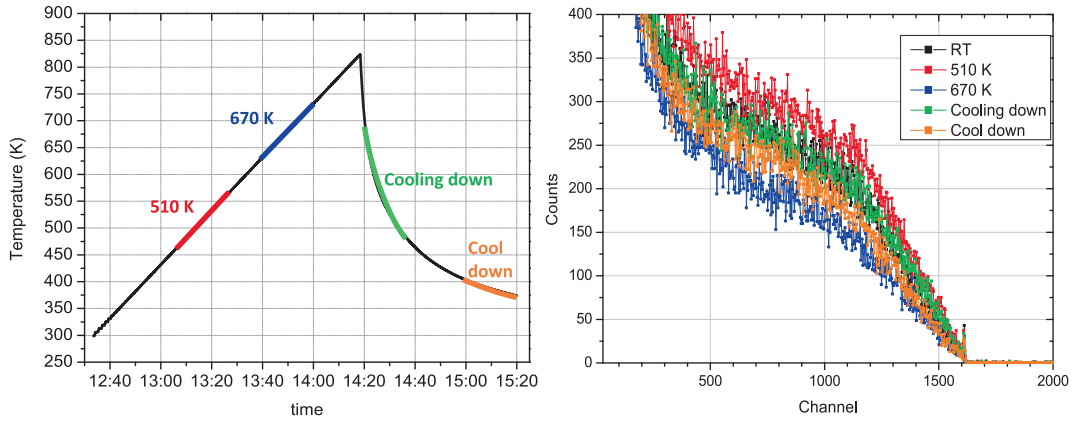

Fig. 6. Left: heating ramp profile and timing of spectra acquisition. time-temperature diagram showing when each rbs spectrum was recorded during the annealing experiment. the mean temperature during the measurement is written. right: rbs-c spectra obtained on the 0.2 dpa, 290 K sample in < 111 > axial channeling direction recorded at RT, 510 K, 670 K, cooling phase, and cool down. The mean temperatures during the spectrum recording are used to label the spectra.

channeling conditions for the beam [21].

The next spectrum, recorded during the cooling stage (green), exhibited an RBS-C yield similar to that at room temperature (black), most likely due to residual thermal vibrations still present in the crystal. After the sample was cooled, the final spectrum (orange) was acquired, showing a reduction in RBS-C yield relative to the initial room-temperature spectrum.

A direct comparison between the 670 K (blue) and the final cooled-down (orange) spectra is not straightforward. Although the contribution due the thermal vibration of the crystal atoms is reduced, a third factor, the radiation from the heating plate, may still have played an important role, and could have affected the measurement, leading to a slightly higher apparent yield for the cooled-down (orange) spectrum compared to the 670 K (blue) spectrum.

If we compare the spectra just after the surface peak, they lay more or less on top of each other, from which we conclude that there was no goniometer sample-angle shift during the heating or cooling cycle. Otherwise, a substantial increase in the RBS-C yield would have been observed.

For this reason, to provide a physical interpretation of what happened during the annealing, and considering the issues with the detector, further characterization studies would be required to conclude that defect annealing was taking place.

In order to achieve a reliable annealing study by RBS-C, we learned that longer waiting times after cooling down would be needed to reduce the effect of light on the detector. Moreover, improved detector protection from the light would be required, for instance by covering the heater or additionally by placing a thin Al foil in front of the detector. However, in this latter case, the detector energy resolution would decrease, and it should therefore be verified whether the RBS-C sensitivity to defect recovery is maintained. From the present results, we can conclude that with the additional light shielding, RBS-C could be successfully employed for *in operando* studies of defect annealing.

4. Discussion and conclusions

4.1. Performance of the new goniometer system

The commissioning measurements demonstrate that the 5-axis high-precision goniometer, at the INSIBA end-station, significantly enhances the capability to perform advanced ion-beam channeling studies on crystalline materials. Its mechanical stability, angular resolution, and temperature control enable measurements that were previously not possible at JSI.

The comparison with benchmark RBS-C and NRA-C data obtained at Madrid and HZDR confirms the excellent alignment accuracy and reproducibility of the new system. The channeling minima (2–3% for pristine W crystals), achieved after the beam-line upgrade and improved beam collimation, are fully consistent with state-of-the-art channeling facilities and good crystallinity samples. The ability to acquire simultaneous RBS-C and NRA-C spectra using two independent detectors with stable geometry demonstrates the quality of the channeling condition, and presents advantages in comparison to other set ups where the same detector is used to collect both signals, with the consequent overlapping of signals. Moreover our 1500 μm thick NRA detector allows absolute quantification of deuterium by fully stopping protons from the D(^{3}He, p)^{4}He reaction, an important capability for fusion-related materials.

The goniometer also provides integrated thermal control, allowing sample heating up to 1470 K, liquid-nitrogen cooling, and electrical bias. This versatility broadens the experimental scope of the facility, enabling studies of irradiation-enhanced diffusion, defect migration, and temperature-dependent trapping phenomena.

4.2. Application to defect Characterisation depth resolution

The ability of the goniometer to resolve irradiation-induced defect structures was validated through RBS-C measurements on pristine and self-irradiated W(111) and W(100) crystals. The depth-resolved signatures of defects, (changes in the slope of the disorder profile, clear knee positions, and dose-dependent increases in dechanneling yield) were all collected with high signal-to-noise ratio. The extracted damage-depth values were consistent with TEM analysis, confirming that the system provides reliable depth resolution.

4.3. Integration of RBS-C and NRA-C for Defect–Hydrogen correlation

The capability of the setup to perform combined RBS-C/NRA-C scans provided direct correlation between lattice disorder and deuterium trapping. The NRA-C angular distributions exhibited the expected broadening and amplitude changes linked to vacancy clustering, confirming that the system can simultaneously track structural defects and hydrogen retention behaviour. This dual-modality capability is particularly valuable for studies of plasma-facing materials, where hydrogen-defect interactions govern fuel retention, embrittlement, and long-term component performance.

4.4. In-situ thermal annealing capability

A main advancement introduced by the new goniometer is the ability to perform in-situ channeling measurements during controlled heating. The system maintained stable alignment during temperature ramps up to ~ 820 K, allowing direct observation of temperature-dependent

defect recovery in the backscattering yield.

The annealing sequence clearly showed the expected competition between thermal vibrations and defect recovery. A small increase in backscattering yield was detected near 510 K, attributed to enhanced lattice vibrations and the corresponding reduction in channeling efficiency. A decrease in RBS-C yield around 670 K was observed, corresponding to damage recovery in tungsten, confirming that the system can resolve thermally activated processes in real time. Although detector light sensitivity currently limits measurements above ~ 800 K, the obtained data demonstrate that in-operando defect evolution studies are now routinely achievable at JSI. Planned improvements in detector shielding are expected to extend the accessible temperature range in future work.

4.5. Conclusion and Outlook

A new high-precision goniometer system has been successfully commissioned at the INSIBA end-station of JSI, representing a major upgrade of the ion-beam analysis infrastructure. The system demonstrated excellent performance in the defect characterization of irradiated tungsten, reliably resolving depth-dependent disorder, and thermally activated defect recovery during in-situ annealing.

The capability for simultaneous RBS-C and NRA-C measurements enables direct correlation between structural defects and deuterium trapping, providing a powerful experimental approach for fusion-materials research. The goniometer offers exceptional alignment accuracy, mechanical stability, and thermal control, allowing the acquisition of high-quality channeling data with well-defined channeling minima and signal-to-noise ratios comparable to leading international facilities.

Its precision, multi-detector configuration, and temperature-control capabilities support advanced channeling studies on single crystals and irradiated materials, including depth-resolved defect quantification, combined structural (RBS-C) and light-element lattice-location (NRA-C) analysis, as well as in-situ annealing and cryogenic irradiation experiments with excellent alignment stability.

Overall, the new goniometer transforms the INSIBA end-station into a modern and versatile platform for advanced *in operando* ion-beam channeling experiments. It establishes a solid experimental foundation for future studies of defect dynamics, hydrogen trapping, and temperature-dependent recovery processes in tungsten and other fusion-relevant materials, while also enabling benchmarking of atomistic simulations and validation of radiation-damage models. The system will further support expanded collaborative research and high-quality experimental and theoretical comparisons.

Declaration of competing interest

The authors declare that they have no known competing financial interests or personal relationships that could have appeared to influence the work reported in this paper.

Acknowledgments

We would like to thank to a group of people from Max-PlanckInstitut für Plasmaphysik, Garching Germany, namely, T. Schwarz-Selinger, J. Dorner and M. Fußeder for W irradiation of the samples and D plasma exposure. Special thanks to K. Hunger for diligent work on polishing the samples and Dr. M. Zibrov for providing tungsten (100) single crystals.

This work has been carried out within the framework of the EUROfusion Consortium, funded by the European Union via the Euratom Research and Training Programme (Grant Agreement No 101052200 EUROfusion). Views and opinions expressed are however those of the author(s) only and do not necessarily reflect those of the European Union or the European Commission. Neither the European Union nor the European Commission can be held responsible for them. Work was performed under Enabling research project DeHydroC project (Detection of Defects and Hydrogen by Ion Beam Analysis in Channelling Mode for Fusion, (CfP-FSD-AWP21-ENR-02-JSI-01).The authors acknowledge the support from the Slovenian Research Agency (research core funding No. P2-0405 and research projects No. J2-3038 and J2-60052).

References

[1] L. Feldman, J. Mayer, S. Picraux, Material Analysis by Ion Channeling, Academic Press, New York, 1982.
[2] A. Vantomme, 50 years of ion channeling in materials science, Nucl. Instrum. Methods Phys. Res., Sect. B 371 (2016) 12–26.
[3] O. Ogorodnikova, V. Gann, Simulation of neutron-induced damage in tungsten by irradiation with, J. Nucl. Mater. 460 (2015) 60–71.
[4] B. Wielunska, M. Mayer, T. Schwarz-Selinger, A. Sand and W. Jacob, "Deuterium retention in tungsten irradiated by different ions," *Nuclear Fision,* vol. 60, no. 9, p. 14pp, 2020.
[5] X. Jin, F. Djurabekova, E.A. Hodille, S. Markelj, K. Nordlund, Analysis of lattice locations of deuterium in tugnsten and its application for predicting deuterium trapping conditions, Phys. Rev. Mater. 8 (2024).
[6] T. Schwarz-Selinger, "A critical review of experiments on deuterium retention in displacement-damaged tungsten as function of damaging dose," *Materials Research Express,* vol. 10, no. 10, 2023.
[7] M. El Bouanani, P. Pelicon, A. Razpet, I. Čadež, M. Budnar, J. Simčič, S. Markelj, Simple and accurate spectra normalization in ion beam analysis using a transmission mesh-based charge integration, Nucl. Inst. Methods Phys. Res. B 243 (2006) 392–396.
[8] S. Markelj, X. Jin, F. Djurabekova, J. Zavašnik, E. Punzón-Quijorna, T. Schwarz-Selinger, M. Crespillo, G. García López, F. Granberg, E. Lu, K. Nordlund, A. Šestan and M. Kelemen, "Unveiling the radiation-induced defect production and damage evolution in tungsten using multi-energy Rutherford backscattering spectroscopy in channeling configuration," *Acta Materialia,* vol. 263, 2024.
[9] J. Zavašnik , A. Šestan, T. Schwarz-Selinger, K. Hunger, E. Lu, F. Tuomisto, K. Nordlund, E. Punzón-Quijorna, M. Kelemen, J. Pedrag, M. Crespillo, G. García López, P. Zhang, X. Cao and S. Markelj, "Microstructural analysis of tungsten single crystals irradiated by MeV W ions: The effect of irradiation dose and temperature," *Materials Characterization,* vol. 224, no. 115050, 2025.
[10] S. Markelj, E. Punzón-Quijorna, M. Kelemen, T. Schwarz-Selinger, R. Heller, X. Jin, F. Djurabekova, E. Lu, J. Predrag, First study of the location of deuterium in displacement-damaged tungsten by nuclear reaction analysis in channeling configuration, Nucl. Mater. Energy 39 (2024).
[11] K. Nordlund, F. Djurabekova, G. Hobler, Large fraction of crystal directions leads to ion channeling, Phys. Rev. B 94 (2016) 214109.
[12] H.-D. Cabstanjen, "Interstitial positions and vibrational amplitudes of hydrogen in metals investigated by fast ion channeling," *Physica Status Solidi (a) applications and Materials*, Science 59 (1) (1980) 11–26.
[13] B. Wielunska, M. Mayer, T. Schwarz-Selinger, U. von Toussaint, J. Bauer, Cross section data for the D(3He,p)4He nuclear reaction from 0.25 to 6 MeV, Nucl. Instrum. Methods Phys. Res., Sect. B 371 (2016) 41–45.
[14] R. Galende, Development of ion beam technique for detection of displacement damage in materials, Master thesis, University Ljubljana, Ljubljana, 2024.
[15] M. Mayer, SIMNRA, a simulation program for the analysis of NRA, RBS and ERDA, AIP. Preceedings (1999) 541–544.
[16] W.-K. Chu, J.W. Mayer, M.-A. Nicolet, Backscattering Spectrometry, New York, San Francisco, Academic Press, London, 1978.
[17] K. Jin, G. Velisa, H. Xue, T. Yang, H. Bei, W.J. Weber, L. Wang, Y. Zhang, Channeling analysis in studing ion irradiation damage in materials containing various types of defects, J. Nucl. Mater. 517 (2019) 9–16.
[18] A. Bruncrona, J. Wu, X. Jin, J. Byggmästar and F. Granberg, "Understanding the RBS/c spectra of irradiated tungsten: A computational study," *Computational Material Science,* vol. 244, no. 113241, 2024.
[19] S. Markelj, J. Zavašnik, A. Šestan, T. Schwarz-Selinger, M. Kelemen, E. Punzón-Quijorna, G. Alberti, M. Passoni, D. Dellasega, Deuterium retention and transport in ion-irradiated tungsten exposed to deuterium atoms: Role of grain boundaries, Nucl. Mater. Energy 38 (2024) 101589.
[20] S. Markelj T. Schwarz-Selinger M. Pečovnik A. Založnik M. Kelemen I. Čadež J. Bauer P. Pelicon W. Chromiński L. Ciupinski Displacement damage stabilization by hydrogen presence under simultaneous W ion damage and D ion exposure Nucl. Fusion 59, Number 8 2019 59(8), pp. 086050.
[21] S. Wang, H. Wang, X. Yi, W. Tan, L. Ge, Y. Sun, W. Gou, Q. Yang, L. Cheng, X. Zhang, Y. Yuan, X. Cao, E. Fu, G.-H. Lu, Damage recovery stages revisited: thermal evolution of non-saturated and saturated displacement damage in heavy-ion irradiated tungsten, Acta Mater. 273 (2024).